Green Synthesis and Catalysis xxx (xxxx) xxx

Contents lists available at ScienceDirect

Green Synthesis and Catalysis

journal homepage: www.keaipublishing.com/en/journals/green-synthesis-and-catalysis

Graphene oxide in palladium nanoparticle (GrafeoPlad): A new class of functional materials

Matteo Formenti [a], Mario Pagliaro [b], Cristina Della Pina [a,**], Rosaria Ciriminna [b,*]

[a] Dipartimento di Chimica, Università degli Studi di Milano, via Golgi 19, 20133 Milano, Italy
[b] Istituto per lo Studio dei Materiali Nananostrutturati, CNR, via U. La Malfa 153, 90146 Palermo, Italy

ARTICLE INFO

Keywords:
MORALs
Palladium
Molecularly doped metal
GrafeoPlad
Graphene oxide

ABSTRACT

Water-soluble graphene oxide was encapsulated within the lattice of Pd nanoparticles using Zn as reducing agent affording a completely new class of functional materials dubbed herein "GrafeoPlad" for designating platinum-group metals doped with 3D entrapped graphene oxide. The first application of this new metal-organic alloy reported herein is in catalysis to convert nitrobenzene to analine with hydrazine as reducing agent at room temperature. GrafeoPlad-Pd is significantly more stable than Pd black showing that the entrapment of GO molecules in the nanoparticle lattice largely improves both its catalytic activity and stability against catalytic deactivation. This new class of hybrid materials may open practically relevant new avenues in many areas of today's material science and technology.

1. Introduction

Consisting of organic molecules 3D entrapped in the lattice structure of metal crystals, organically doped metals were introduced by Avnir in 2002 reporting the entrapment of Congo Red dye in silver [1]. As simple as effective, the method involves concomitant dissolution in water of a metal salt precursor and of the dopant organic molecules, followed by reduction of the metal cations with a reducing agent [2,3]. Employing a surfactant, the method was readily demonstrated to be effective also for the entrapment of water-insoluble organic molecules [1]. In 2008 Avnir's team also demonstrated the successful encapsulation of polymers in Cu and in Ag either by emulsifying the dopant molecules in water with a surfactant or by utilizing a solvent such as dimethylformamide [4]. The subsequent year, reporting the encapsulation of Cu(II) and Fe(III) phthalocyanines in Ag nanoparticles, Pagliaro and co-workers dubbed these materials "metal-organic alloys" (MORALs) [5]. Today, the applications of MORALs range from ionomer@Ag for enhanced electrocatalytic anion-exchange membranes for hydrogen fuel cells [6] through alkaloid@Cu for highly selective, waste-free, electrocatalytic asymmetric ketone hydrogenations [7]. A recent insight on practical aspects concerning the use of MORALs in catalysis concluded that supported molecularly doped metals will be especially used in continuous flow processes [8].

Graphene has been widely studied as reinforcing material in different metal/graphene composite materials (generally made by mixing, compacting and sintering or by extrusion) [9]. For instance, graphene coated on both sides of a Cu foil *via* a chemical vapor deposition (followed by stacking and hot pressing numerous layers of numerous Gr/Cu/Gr foils) affords copper having an electrical conductivity 117% higher than pure copper [10]. Other applications include the use of graphene oxide as support of Pd nanoparticles [11], or of single metal atoms [12] for catalytic applications. Now, reporting the encapsulation of graphene oxide (GO) in palladium nanoparticles (NPs), we introduce a completely new class of functional materials dubbed herein "GrafeoPlad" for designating platinum group metals (PGMs) doped with 3D entrapped GO.

2. Results and discussion

Depicted in Scheme 1, the catalyst synthesis goes through the employment of water-soluble graphene oxide.

The TEM photographs of GrafeoPlad-Pd in Fig. 1 show that the material is comprised of aggregated palladium nanoparticles (Fig. 1a and d,e), some of which clearly reveal the presence of glassy GO layers on the edge of the aggregated NPs (Fig. 1b and c,f). In other parts, the Pd aggregated nanoparticles are tightly intertwined with GO regions (Fig. 1a and d,e).

* Corresponding author.
** Corresponding author.
E-mail addresses: cristina.dellapina@unimi.it (C. Della Pina), rosaria.ciriminna@cnr.it (R. Ciriminna).

https://doi.org/10.1016/j.gresc.2024.04.004
Received 19 December 2023; Received in revised form 13 March 2024; Accepted 24 April 2024

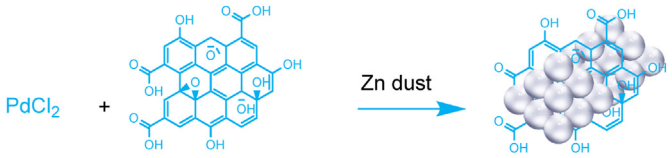

Scheme 1. Synthesis of GO@nPd, palladium-entrapped graphene oxide.

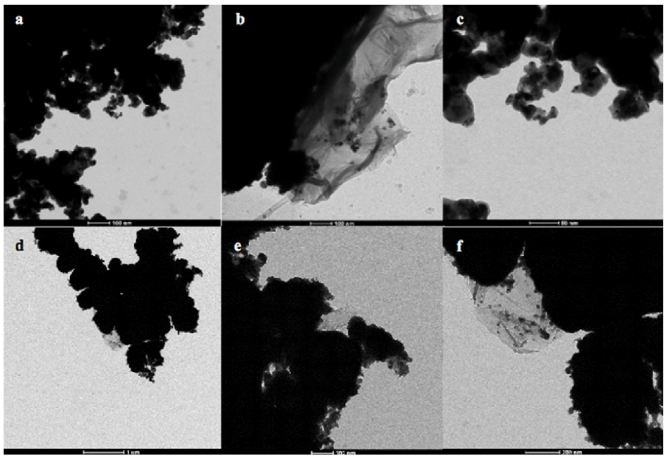

Fig. 1. TEM photographs of fresh GrafeoPlad-Pd (GO@nPd).

Following use of GrafeoPlad-Pd as catalyst to mediate the nitrobenzene reduction to aniline with hydrazine at room temperature (see below), the material retains its structural features (Fig. 2). The regions comprised of tightly aggregated Pd nanoparticles with evidence of graphene-like layers (Fig. 2a and d) are still clearly visible along with others in which more disperse Pd nanoparticles are deposited over GO aggregated layers (Fig. 2b and c, Fig. 2e and f). This is probably due to the disaggregation of some catalyst grain, compatible with the slight loss of activity we see from the time course studies after the first reaction run (see below).

The XRD diffractogram of GrafeoPlad-Pd (Fig. 3) shows evidence that the material consists of graphene oxide entrapped in Pd nanoparticles (GO@nPd). Well-defined peaks around 40° and 46° in the diffractogram originate from the (111) and (200) crystal planes of Pd nanoparticles 9 nm in diameter (derived by the Scherrer equation). The entrapped GO platelets are revealed by the diffraction peak at 13° visible by magnifying the diffraction pattern.

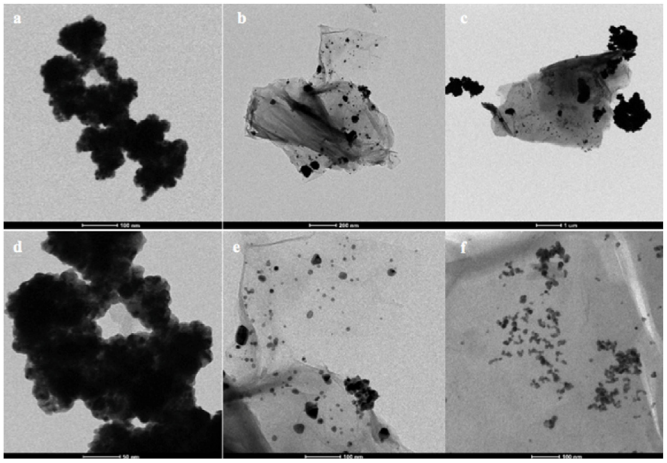

Fig. 2. TEM photographs of GrafeoPlad-Pd (GO@nPd) following its use as catalyst to mediate the nitrobenzene reduction to aniline with hydrazine.

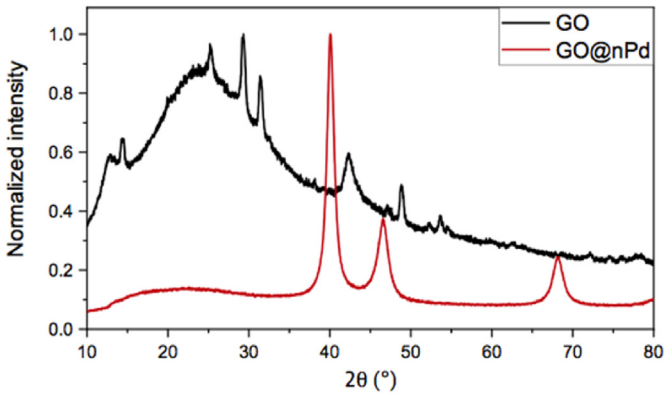

Fig. 3. XRD diffractograms for GO and fresh GO@nPd.

Accordingly, the XRD spectrum for GO shows a peak at 13° and a broad band centered at 24° related to the A–B stacking order, corresponding to the (002) reflection of relatively large reflection (large full width at half maximum), pointing to a relatively low number of layers in the GO sample [12]. Successful encapsulation of the GO layers is shown by the typical infrared "fingertip" bands in the FTIR spectra in Fig. 4.

The spectra of GO@nPd and commercial GO show at 3424 and 3442 cm^{-1} the O–H group stretching vibration peaks. The carboxylic C═O stretching signal of GO at 1721 cm^{-1} disappears in GO@nPd, whereas the signal at 1637 cm^{-1} for GO@nPd is due to ketone group (C═O) shifted to slightly higher wavenumber than in free GO (1627 cm^{-1}) [13].

The asymmetric and symmetric stretching vibrations of CH_2 bonds at 2919 and 2849 cm^{-1}, the C–OH bond stretching frequency at 1380 cm^{-1} (and 1384 cm^{-1} for GO@nPd) and the shoulder peak at 1227 cm^{-1} ascribed to the C–O–C (epoxy group) stretching mode in GO [14], present in both spectra all point to successful entrapment of GO within the Pd nanoparticles.

Finally, further proof of said successful entrapment of GO in the lattice of Pd nanocrystals stems from the X-ray photoelectron spectroscopy (XPS) investigation of GrafeoPlad, that clearly shows all the signals of C 1s components (corresponding to C═C, C–OH, C–O, C═O, and HO–C═O C 1s photoelectrons) characteristic for the particular groups of GO [15]. Furthermore, the high relative abundance of C–OH sp^3 carbons at the surface of Pd-entrapped GO and the relatively low amount of carboxyl groups indicates that the majority of the latter groups in GO are concomitantly reduced during the reduction of Pd^{2+} with Zn leading to precipitation of the MORAL (Scheme 1) [15].

As mentioned above, GrafeoPlad-Pd was employed in nitrobenzene hydrogenation with hydrazine in liquid phase at room temperature. Fig. 5 shows the time course studies of the hydrogenation mediated by GrafeoPlad next to the time course studies of the same reaction mediated

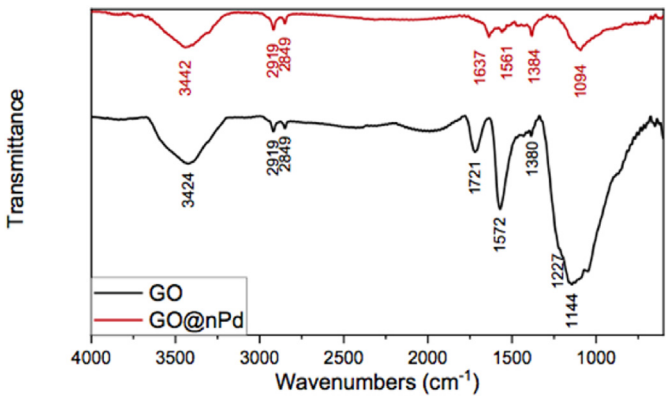

Fig. 4. FTIR spectrum for GO and fresh GO@nPd.

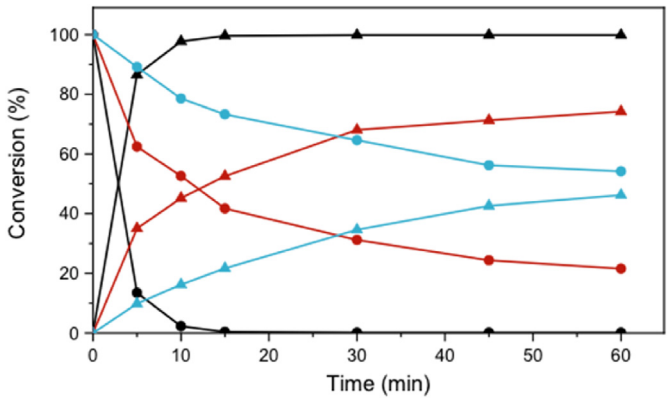

Fig. 5. Time course studies of nitrobenzene (circles) hydrogenation with hydrazine giving aniline (triangles) mediated by GO@nPd (red lines), commercial Pd/C (5 wt%, black lines) and palladium black (blue lines).

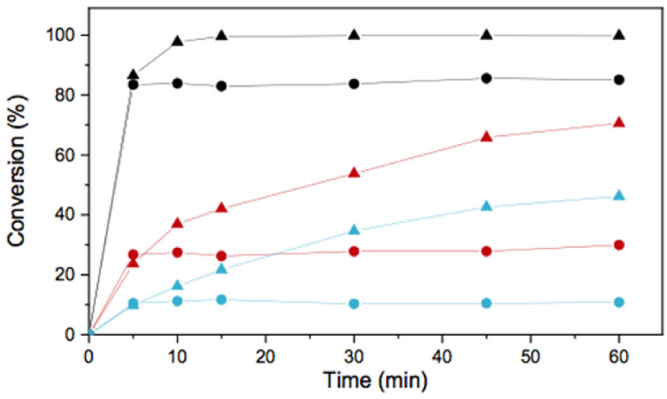

Fig. 6. Activity of the reaction mixture (triangles series) and of reaction filtrate upon removing the catalyst via filtration after 5 min (circle series) using GO@nPd (red lines), Pd/C (black lines) and palladium black (blue lines).

by the commercial Pd/C catalyst and palladium black. All the catalysts selectively afford aniline, with the commercial Pd/C rapidly affording complete conversion of the substrate after 15 min, whereas the conversion of nitrobenzene over GrafeoPlad-Pd after 60 min was about 75%. Palladium black turned out to be the least effective catalyst, affording a 46% nitrobenzene conversion.

Remarkably, the filtration test in which the catalyst is removed by filtration when reaction is not complete (after 5 min, in this case) proved that no active species of Pd are actually leached in solution due to complete absence of reactivity of the reaction filtrate upon filtering the catalyst (Fig. 6).

The GrafeoPlad-Pd catalyst was reusable with only modest loss in activity between the first and the second reaction run (Fig. 7), likely due to adsorption and partial pore blockage of the hydrophilic reactant and product molecules in the inner porosity of the hydrophilic GO@nPd nanoparticles. Moreover, GrafeoPlad-Pd showed a high level of catalyst stability, leading to an almost constant yield despite the initial slight loss in activity after the first run.

Performing reusability tests on all the three catalysts studied (GrafeoPlad-Pd, Pd/C and palladium black, Fig. 8) revealed that commercial Pd/C is more active than GrafeoPlad-Pd in the first three runs, after which it rapidly loses activity, especially after the third and fourth run. On the other hand, palladium black has a relatively low catalytic activity already in the first run, and rapidly loses its activity after the third run.

This shows evidence that the entrapment of GO molecules in the palladium nanoparticle lattice largely improves both its catalytic activity and stability, *de facto* stabilizing Pd nanoparticles against catalytic deactivation, a major achievement in catalysis science and technology due to the large scope of palladium catalysis with Pd nanoparticles in contemporary synthetic organic chemistry.

The FTIR spectra of GrafeoPlad-Pd prior and after mediating the hydrogenation of nitrobenzene with hydrazine (Fig. 9) show that the signal of carbonyl groups (1637 cm^{-1}) decreases, whereas the signal due to the C–OH bond stretching frequency at 1384 cm^{-1} sharpens. This outcome may be due to the Pd nanoparticles embedding the GO layers of GrafeoPlad-Pd catalyzing the reduction of graphene oxide carbonyl groups to alcoholic functions. We remind that the reduction of GO to reduced graphene oxide (RGO) with hydrazine requires prolonged (3 h) treatment of GO at 95 °C [16]. We hypothesize that the good catalytic activity of GO@nPd may be due to the electron donation from the extensive π-π bonds in the hexagonal carbon lattice of the graphene oxide to the unoccupied orbitals of Pd nanoparticles, as it happens with the enhanced catalytic activity of Pd towards H_2 chemisorption, with graphene acting both as an electron reservoir and molecular pathway [17].

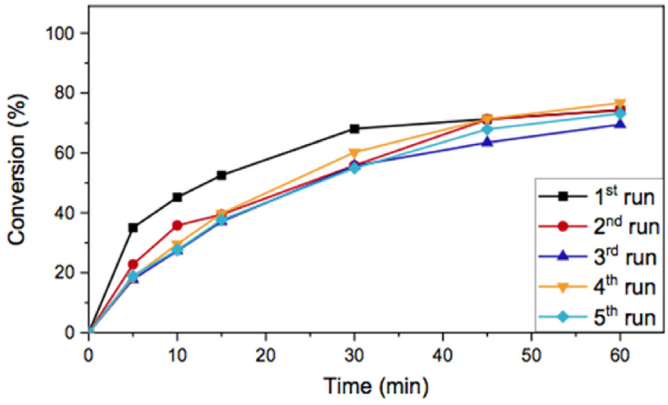

Fig. 7. Conversion of nitrobenzene to aniline mediated by GO@nPd in five consecutive reduction runs.

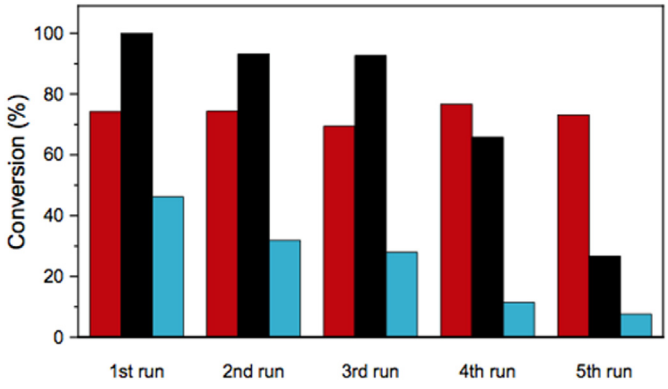

Fig. 8. Comparison between GrafeoPlad-Pd (red), Pd/C (black) and palladium black (blue) conversions of nitrobenzene to aniline over five consecutive reaction runs.

Previous studies on Pd NPs deposited on GO suggest that the activity of the resulting catalyst is due to the single-layer hydrophilic sheet structure onto which polarized substrates such as arylboronic acids easily adsorb and from which the less polarized biphenyl products can readily dissociate [18]. GO and Pd/GO nanosheets, however, tend to self-assemble at relatively higher concentrations and temperatures, especially in aqueous media, requiring exfoliation of the GO sheets by surfactants to enhance the catalytic activity of the used Pd/GO catalyst [18].

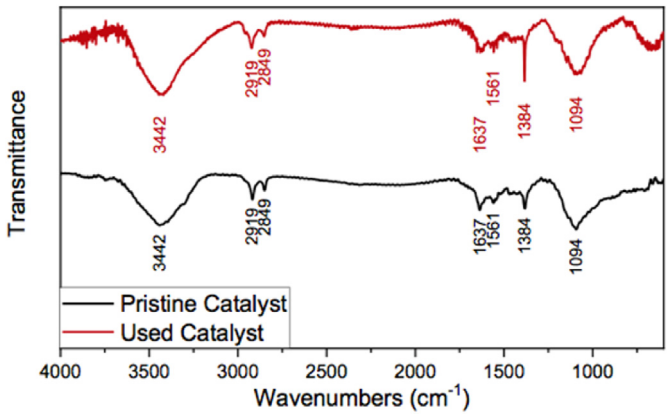

Fig. 9. FTIR spectrum for GO@nPd after mediating the reaction of nitrobenzene with excess hydrazine.

3. Conclusions

In conclusion, we have discovered that graphene oxide molecules can be effectively entrapped within the crystal lattice of Pd nanoparticles using Avnir's approach to moral organic alloy material synthesis [1–3]. The 3D entrapment of graphene oxide in the crystal lattice of Pd is completely different from the 2D adsorption of Pd nanoparticles on GO, and opens the path to GrafeoPlad-Pd applications in catalysis with even higher efficacy and at substantially lower cost than Pd nanoparticles supported on GO [19], well beyond the catalytic reduction of nitrobenzene to aniline at room temperature reported herein.

For practical applications in which higher activity is required, the GrafeoPlad-Pd nanoparticles will be dispersed on large surface area supports ensuring enhanced accessibility of the reactants to the catalytic active species. The latter approach has been already demonstrated by Avnir and Grader with a MORAL made of Ag entrapping a molecular dye supported on TiO_2 nanotubes to catalyze methanol partial oxidation with unprecedented high activity and catalyst stability [20].

Further investigation of the chemical and physical properties of these new GO@Metal class of metal-organic alloys may open practically relevant new avenues in many areas of today's material science and technology. The findings reported in this study, indeed, are general as shown by the successful entrapment of GO within the lattice of Ni-based nanoparticles for enhanced water electrolysis following the approach first presented herein [21]. Following the approach outlined herein it is possible to encapsulate GO molecules in the crystal lattice of many other metals, including platinum-group metals.

4. Experimental

4.1. Material synthesis

GrafeoPlad-Pd was prepared by adding a solution of 200 mg of palladium chloride (Sigma Aldrich, Milan, Italy) in 50 mL aqueous ethanol (H_2O:EtOH 1:1) kept under stirring with 452 μL of an aqueous solution of GO (8 mg/mL, purchased by Nanografi Nano Teknoloji, Ankara, Turkey). After 30 min stirring, the mixture was added with 86 mg of powdered Zn (Sigma Aldrich, Milan, Italy). The suspension nearly immediately turned to black due to formation of Pd nanoparticles embedding the GO. The mixture was left overnight to ensure complete reduction of Pd^{2+} cations and concomitant entrapment of the GO platelets, after which a solid black precipitate (GrafeoPlad-Pd or GO@nPd, where n stands for "nanoparticle") was filtered through a paper filter (Whatman 5), washed with HCl 0.1 mol/L to remove the excess of Zn and dried overnight at 40 °C in an oven.

4.2. Structural characterization

The transmission electron microscopy (TEM) experiments were carried out using a Thermo Fisher Scientific Talos L120C instrument operating at 120 kV. Samples were deposited on Cu-grids as such. The XRD diffractograms were obtained using a Rigaku Miniflex 600 diffractometer with Cu Kα radiation ($\lambda = 0.1541$ nm), acquiring data in the 10–80° 2θ range with a step size of 0.05° and a counting time of 8 s per step. The FTIR spectra were recorded with a JASCO FT/IT 4100 instrument, preparing the samples in KBr pellets, acquiring data in the 4000-600 cm^{-1} range.

4.3. Catalytic reactions

The catalytic reduction of nitrobenzene (99% purity, Sigma Aldrich, Milan) was carried out at room temperature using hydrazine hydrate (85% solution, Carlo Erba, Milan). In a typical reaction, 40 μL of nitrobenzene (3.9×10^{-4} mol) and 46 μL of hydrazine hydrate (8.04×10^{-4} mol) were dissolved in 6 mL of methanol in the presence of 3 mg of GrafeoPlad-Pd. The reaction was also carried out employing a commercial Pd/C (63 mg, 5 wt%) catalyst (Engelhard Italiana, Rome, Italy), containing the same amount of Pd, and 3 mg of Palladium black synthetized in the same way of GrafeoPlad-Pd except for the absence of graphene oxide. In each case, the reaction was monitored via high performance liquid chromatography (HPLC) using a Shimadzu LC-10ADvp (Shimadzu Corporation, Kyoto, Japan) chromathograph equipped with a RID-10A detector and Restek Ultra BiPh 5 μm column (Restek, Cernusco sul Naviglio, Italy). A H_2O:MeOH 1:1 solution was the eluent. At the end of the reaction, the catalyst was recovered by centrifugation, washed using ethyl acetate, dried at room temperature and reused as such.

CRediT authorship contribution statement

Matteo Formenti: Validation, Investigation, Data curation. **Mario Pagliaro:** Writing – original draft, Methodology, Conceptualization. **Cristina Della Pina:** Writing – review & editing, Supervision, Methodology, Funding acquisition, Conceptualization. **Rosaria Ciriminna:** Writing – review & editing, Resources, Methodology, Formal analysis, Conceptualization.

Declaration of competing interest

The authors declare that they have no known competing financial interests or personal relationships that could have appeared to influence the work reported in this paper.

Acknowledgements

This study is dedicated to Professor David Avnir on the occasion of his 75th birthday. We thank the Università degli Studi di Milano PSR2021_DIP_005_PI_CDPIN project for funding, and Dr Nadia Santo, Unitech NOLIMITS, Università degli Studi di Milano, for the TEM images.

Appendix A. Supplementary data

Supplementary data to this article can be found online at https://doi.org/10.1016/j.gresc.2024.04.004.

References

[1] H. Behar-Levy, D. Avnir, Chem. Mater. 14 (2002) 1736–1741.
[2] D. Avnir, Acc. Chem. Res. 47 (2014) 579–592.
[3] D. Avnir, Adv. Mater. 30 (2018) 1706804.
[4] G. Nesher, G. Marom, D. Avnir, Chem. Mater. 20 (2008) 4425–4432.

[5] G. Palmisano, V. Augugliaro, R. Ciriminna, M. Pagliaro, Can. J. Chem. 87 (2009) 673–677.
[6] N. Ralbag, M. Mann-Lahav, E.S. Davydova, U. Ash, R. Galed, M. Handl, R. Hiesgen, E. Magliocca, W. Mustain, J. He, P. Cong, A.M. Beale, G.S. Grader, D. Avnir, D.R. Dekel, Matter 1 (2019) 959–975.
[7] H.P. Yang, Q. Fen, H. Wang, J.X. Lu, Electrochem. Commun. 71 (2016) 38–42.
[8] R. Ciriminna, M. Formenti, M. Pagliaro, C. Della Pina, ChemCatChem 15 (2023) e202300600.
[9] Ö. Güler, N. Bağcı, J. Mater. Res. Technol. 9 (2020) 6808–6833.
[10] M. Cao, D. Xiong, L. Yang, S. Li, Y. Xie, Q. Guo, Z. Li, H. Adams, J. Gu, T. Fan, X. Zhang, D. Zhang, Adv. Funct. Mater. 29 (2019) 1806792.
[11] X. Chen, G. Wu, J. Chen, X. Chen, Z. Xie, X. Wang, J. Am. Chem. Soc. 133 (2011) 3693–3695.
[12] J.B. Liu, H.S. Gong, G.L. Ye, H.L. Fei, Rare Met. 41 (2022) 1703–1726.
[13] G. Surekha, K.V. Krishnaiah, N. Ravi, R. Padma Suvarna, J. Phys. Conf. Ser 1495 (2020) 012012.
[14] S. Chaiyakun Rattana, N. Witit-anun, N. Nuntawong, P. Chindaudom, S. Oaew, C. Kedkeaw, P. Limsuwan, Procedia Eng. 32 (2012) 759–764.
[15] M. Formenti, M.P. Casaletto, G. Barone, M. Pagliaro, C. Della Pina, V. Butera, R. Ciriminna, Adv. Sust. Syst. 8 (2024) 2300643.
[16] P.G. Ren, D.X. Yan, X. Ji, T. Chen, Z.M. Li, Nanotechnology 22 (2011) 055705.
[17] X. Tang, P.A. Haddad, N. Mager, X. Geng, N. Reckinger, S. Hermans, M. Debliquy, J.P. Raskin, Sci. Rep. 9 (2019) 3653.
[18] S. Rostamnia, B. Zeynizadeh, E. Doustkhah, H.G. Hosseini, J. Colloid Interface Sci. 451 (2015) 46–52.
[19] B.F. Machado, P. Serp, Catal. Sci. Technol. 2 (2012) 54–75.
[20] Y. Aouat, G. Marom, D. Avnir, V. Gelman, G.E. Shter, G.S. Grader, J. Phys. Chem. C 117 (2013) 22325–22330.
[21] M. Pagliaro, M.V. Pagliaro, R. Caliandro, C. Giannini, R. Ciriminna, A. Lavacchi, Mater. Adv. 5 (2024) 2759–2766.